Ann. Inst. H. Poincaré D
Comb. Phys. Interact. 9 (2022), 47–72
DOI 10.4171/AIHPD/113

Nested Catalan tables and a recurrence relation in noncommutative quantum field theory

Jins de Jong, Alexander Hock, and Raimar Wulkenhaar

Abstract. Correlation functions in a dynamic quartic matrix model are obtained from the two-point function through a recurrence relation. This paper gives the explicit solution of the recurrence by mapping it bijectively to a two-fold nested combinatorial structure each counted by Catalan numbers. These "nested Catalan tables" have a description as diagrams of non-crossing chords and threads.

1. Introduction

The quartic matrix model is defined by the following measure on the space of self-adjoint $\mathcal{N} \times \mathcal{N}$-matrices:

$$\mathrm{d}\,\mu(\Phi) = \frac{1}{\mathcal{Z}} \exp\Big(-\mathcal{N}\,\mathrm{Tr}\Big(E\Phi^2 + \frac{\lambda}{4}\Phi^4 \Big)\Big)\,\mathrm{d}\,\Phi, \tag{1}$$

where $E = \mathrm{diag}(E_0, \ldots, E_{\mathcal{N}-1})$ is a positive $\mathcal{N} \times \mathcal{N}$-matrix, λ a scalar and $\mathrm{d}\,\Phi$ the standard Lebesgue measure. The measure (1) gives rise to moments

$$\langle a_1 b_1; \ldots; a_N b_N \rangle := \int \mathrm{d}\,\mu(\Phi) \Phi_{a_1 b_1} \Phi_{a_2 b_2} \cdots \Phi_{a_N b_N}$$

which decompose as usual into cumulants $\langle a_1 b_1; \ldots; a_N b_N \rangle_c$.

This matrix model arises from a programme to understand Euclidean quantum fields on noncommutative spaces [18]. The large-$\mathcal{N}$ limit of properly rescaled cumulants $\langle a_1 b_1; \ldots; a_N b_N \rangle_c$, in a suitable topology, leads to the same challenges as in familiar quantum field theories concerning renormalisation and existence for $\lambda \neq 0$. It turned out that for the matrix model the challenges are easier to master. Consider cumulants with pairwise different a_i. Then $\langle a_1 b_1; \ldots; a_N b_N \rangle_c$ is only non-vanishing

2020 Mathematics Subject Classification. Primary 05A19; Secondary 05C30, 81R60.
Keywords. Catalan numbers, chord diagrams, noncommutative QFT.

if N is even and $b_i = a_{\pi(i)}$ for some permutation $\pi \in \mathcal{S}_N$. If $c(\pi)$ is the number of cycles in π, we expand

$$\mathcal{N}^N \langle a_1 b_{\pi(1)}; \dots ; a_N b_{\pi(N)} \rangle_c =: \sum_{g=0}^{\infty} \mathcal{N}^{2-2g-c(\pi)} G^{(g,\pi)}_{a_1 \dots, a_N}. \tag{2}$$

This paper is part of the programme to construct functions $Z(\mathcal{N}, \lambda)$, $\mu^2(\mathcal{N}, \lambda)$ such that when starting from (1) with

$$E_k \mapsto Z(\mathcal{N}, \lambda)\Big(E_k + \frac{1}{2}\mu^2(\mathcal{N}, \lambda)\Big), \quad \lambda \mapsto (Z(\mathcal{N}, \lambda))^2 \lambda,$$

every limit $\lim_{\mathcal{N}\to\infty} G^{(g,\pi)}_{a_1 \dots a_N}$ exists in a neighbourhood of $\lambda = 0$.

The first step consists in understanding the case where π has a single cycle $c(\pi) = 1$ and in leading order $g = 0$ of the $1/\mathcal{N}$-expansion. We relabel the indices to achieve $b_i = a_{i+1}$ (with $b_0 \equiv b_N$) and write $G^{(0,\pi(i)=i+1)}_{a_1 \dots a_N} = G^{(0)}_{b_0 \dots b_{N-1}}$. For these functions the following recurrence relation was proved in [10]:

$$G^{(0)}_{b_0 \dots b_{N-1}} = -\lambda \sum_{l=1}^{\frac{N-2}{2}} \frac{G^{(0)}_{b_0 \dots b_{2l-1}} \cdot G^{(0)}_{b_{2l} \dots b_{N-1}} - G^{(0)}_{b_1 \dots b_{2l}} \cdot G^{(0)}_{b_0 b_{2l+1} \dots b_{N-1}}}{(E_{b_0} - E_{b_{2l}})(E_{b_1} - E_{b_{N-1}})}. \tag{3}$$

Equation (3) is the counterpart of *Tutte equations* arising in the enumeration of maps on surfaces [17] or of *loop equations* in matrix models [5]. The recurrence relation (3) is specific to the measure (1); Dyson–Schwinger techniques and $U(\mathcal{N})$ invariance of the partition function are used to prove it. The planar 2-point function $G^{(0)}_{b_0 b_1}$ satisfies a closed non-linear equation [9] which was solved in [13] for a limiting case of linearly spaced $E_k = (c_0 + kc_1)$.

In this paper we establish a bijection between the solution of (3) and a combinatorial problem for two nested structures each counted by Catalan numbers. We thus propose to name them “nested Catalan tables.” As by-product we observed that the same relation (3) appears in the planar sector of the 2-matrix model for mixed correlation functions [6]. The distinction between even b_{2i} and odd b_{2i+1} matrix indices in (3) corresponds to the different matrices of the 2-matrix model. This observation together with a striking rôle of an involution in [13] supported the conjecture that also the quartic matrix model (1) relates to topological recursion [5,7]. This vision led two of us (A. Hock and R. Wulkenhaar) together with H. Grosse in [8] to an exact solution $G^{(0)}_{b_0 b_1}$ of the non-linear equation [9] for arbitrary E_k and λ in or near $\mathbb{R}_+$. Together with results of this paper we thus have a complete understanding of the cumulants $G^{(0,\pi(i)=i+1)}_{a_1 \dots a_N} = G^{(0)}_{b_0 \dots b_{N-1}}$ in leading $\frac{1}{\mathcal{N}}$-order. In the meantime a precise relation between (1) and blobbed topological recursion [1] was established in [2, 3, 11]. This means that the quartic matrix model generates the combinatorics of a family of intersection numbers of characteristic classes on the moduli space $\bar{\mathcal{M}}_{g,n}$ of stable complex curves.

Let us return to the recurrence relation (3) and explain the combinatorial problem. For this purpose it is safe to consider the $\{E_{b_j}\}$ as pairwise different formal variables and to set $\lambda = -1$. The complete expression for the $(N = 2k + 2)$-point function $G^{(0)}_{b_0 b_1 \dots b_{2k+1}}$ according to (3) yields $2^k c_k$ terms of the form

$$\frac{\pm G^{(0)}_{b_p b_q} \cdots G^{(0)}_{b_r b_s}}{(E_{b_t} - E_{b_u}) \cdots (E_{b_v} - E_{b_w})} \tag{4}$$

with $p < q$, $r < s$, $t < u$ and $v < w$, where $c_k = \frac{1}{k+1}\binom{2k}{k}$ is the k-th Catalan number. However, some of the terms cancel. In this paper we answer the so far open questions: *Which terms survive the cancellations? Can they be explicitly characterised, without going into the recursion?* The answer will be encoded in *nested Catalan tables*.

The paper is organised as follows. In Section 2 the symmetries of $G^{(0)}_{b_0 \dots b_{N-1}}$ are discussed. Afterwards, in Sections 3 and 4 we introduce Catalan tuples, nested Catalan tables, certain trees and operations on them. The Catalan numbers $c_k = \frac{1}{k+1}\binom{2k}{k}$ will count various parts of our results and will be related to the number $d_k = \frac{1}{k+1}\binom{3k+1}{k}$ of nested Catalan tables of length $k + 1$, see Proposition 4.4. Section 5 is the main part of this paper. We prove in Theorem 5.5 that nested Catalan tables precisely encode the surviving terms in the expansion of $G^{(0)}_{b_0 \dots b_{N-1}}$ with specified designated node.

Both the nested Catalan tables and the $G^{(0)}_{b_0 \dots b_{N-1}}$ can be depicted conveniently as chord diagrams with threads, which will be introduced in Appendix B. Through these diagrams it will become clear that the recursion relation (3) is related to well-known combinatorial problems [4, 12].

2. Symmetries

The two-point function is symmetric, $G^{(0)}_{b_p b_q} = G^{(0)}_{b_q b_p}$. Because there is an even number of antisymmetric factors in the denominator of each term, it follows immediately that

$$G^{(0)}_{b_0 b_1 \dots b_{N-1}} = G^{(0)}_{b_{N-1} \dots b_1 b_0}. \tag{5}$$

Our aim is to prove cyclic invariance $G^{(0)}_{b_0 b_1 \dots b_{N-1}} = G^{(0)}_{b_1 \dots b_{N-1} b_0}$. We proceed by induction. Assuming that all n-point functions with $n \leq N - 2$ are cyclically invariant, it is not difficult to check that

$$
\begin{aligned}
&G^{(0)}_{b_0 b_1 \dots b_{N-1}} \\
&= \sum_{l=1}^{\frac{N-2}{2}} \frac{G^{(0)}_{b_0 \dots b_{2l-1}} \cdot G^{(0)}_{b_{2l} \dots b_{N-1}} - G^{(0)}_{b_1 \dots b_{2l}} \cdot G^{(0)}_{b_0 b_{2l+1} \dots b_{N-1}}}{(E_{b_0} - E_{b_{2l}})(E_{b_1} - E_{b_{N-1}})} \\
&= -\sum_{l=1}^{\frac{N-2}{2}} \frac{G^{(0)}_{b_0 b_{N-1} \dots b_{2l+1}} \cdot G^{(0)}_{b_{2l} \dots b_1} - G^{(0)}_{b_{N-1} \dots b_{2l}} \cdot G^{(0)}_{b_{2l-1} \dots b_1 b_0}}{(E_{b_0} - E_{b_{2l}})(E_{b_1} - E_{b_{N-1}})} \\
&= \sum_{k=1}^{\frac{N-2}{2}} \frac{G^{(0)}_{b_0 b_{N-1} \dots b_{N-2k+1}} \cdot G^{(0)}_{b_{N-2k} \dots b_1} - G^{(0)}_{b_{N-1} \dots b_{N-2k}} \cdot G^{(0)}_{b_0 b_{N-2k-1} \dots b_1}}{(E_{b_0} - E_{b_{N-2k}})(E_{b_{N-1}} - E_{b_1})} \\
&= G^{(0)}_{b_0 b_{N-1} \dots b_1} = G^{(0)}_{b_1 \dots b_{N-1} b_0}. \qquad (6)
\end{aligned}
$$

The transformation $2l = N - 2k$ and the symmetry (5) are applied here to rewrite the sum. This shows cyclic invariance.

Although the N-point functions are invariant under a cyclic permutation of its indices, the preferred expansion into surving terms (4) will depend on the choice of a designated node b_0, the root. Our preferred expansion will have a clear combinatorial significance, but it cannot be unique because of

$$
\frac{1}{E_{b_p} - E_{b_q}} \cdot \frac{1}{E_{b_q} - E_{b_r}} + \frac{1}{E_{b_r} - E_{b_p}} \cdot \frac{1}{E_{b_p} - E_{b_q}} + \frac{1}{E_{b_q} - E_{b_r}} \cdot \frac{1}{E_{b_r} - E_{b_p}} = 0. \qquad (7)
$$

These identities must be employed several times to establish cyclic invariance of our preferred expansion.

3. Catalan tuples

Definition 3.1 (Catalan tuple). A Catalan tuple $\tilde{e} = (e_0, \dots, e_k)$ of length $k \in \mathbb{N}_0$ is a tuple of integers $e_j \geq 0$ for $j = 0, \dots, k$, such that

$$
\sum_{j=0}^{k} e_j = k \quad \text{and} \quad \sum_{j=0}^{l} e_j > l \quad \text{for } l = 0, \dots, k-1. \qquad (8)
$$

The set of Catalan tuples of length $|\tilde{e}| := k$ is denoted by $\mathcal{C}_k$.

For $\tilde{e} = (e_0, \dots, e_k)$ it follows immediately that, for all $k \geq 0$, $e_k = 0$ and that, for all $k > 0$, $e_0 > 0$.

Example 3.2. We have $\mathcal{C}_0 = \{(0)\}$, $\mathcal{C}_1 = \{(1, 0)\}$ and $\mathcal{C}_2 = \{(2, 0, 0), (1, 1, 0)\}$. All Catalan tuples of length 3 are given in the first column of Table 1.

Remark 3.3. Catalan tuples can be used to establish bijections with several structures counted by Catalan numbers. In Definitions 3.6 and 3.7 we provide two bijections to planted plane trees. Here we give the bijection to Dyck paths on a $k \times k$ lattice which do not go below the diagonal. Given a Catalan tuple $\tilde{e} = (e_0, \ldots, e_k)$ with $k \geq 1$. Start at the bottom left corner, go e_0 steps north followed by one step east, then go e_1 steps north followed by one step east, ..., finally go e_{k-1} steps north followed by one step east, and stop at the top right corner. The first condition in (8) prevents the path from going below the diagonal, the last condition guarantees that the path ends at the top right corner. The last row of Table 1 gives the Dyck paths for the Catalan tuples of length 3.

We define two particular compositions of Catalan tuples. Appendix A provides a few examples.

Definition 3.4 ($\circ$-composition). The composition $\circ\colon \mathcal{C}_k \times \mathcal{C}_l \to \mathcal{C}_{k+l+1}$ is given by

$$(e_0, \ldots, e_k) \circ (f_0, \ldots, f_l) := (e_0 + 1, e_1, \ldots, e_{k-1}, e_k, f_0, f_1, \ldots, f_l).$$

No information is lost in this composition, i.e., it is possible to uniquely retrieve both terms. In particular, $\circ$ cannot be associative or commutative. Consider for a Catalan tuple $\tilde{e} = (e_0, \ldots, e_k)$ partial sums $p_l\colon \mathcal{C}_k \to \{0, \ldots, k\}$ and maps $\sigma_a\colon \mathcal{C}_k \to \{0, \ldots, k\}$ defined by

$$\begin{aligned} p_l(\tilde{e}) &:= -l + \sum_{j=0}^{l} e_j, \quad \text{for } l = 0, \ldots, k-1, \\ \sigma_a(\tilde{e}) &:= \min\{l \mid p_l(\tilde{e}) = a\}. \end{aligned} \tag{9}$$

Then

$$\tilde{e} = (e_0, \ldots, e_k) = (e_0 - 1, e_1, \ldots, e_{\sigma_1(\tilde{e})}) \circ (e_{\sigma_1(\tilde{e})+1}, \ldots, e_k). \tag{10}$$

Because $\sigma_1(\tilde{e})$ exists for any $\tilde{e} \in \mathcal{C}_k$ with $k \geq 1$, every Catalan tuple has unique $\circ$-factors. Only these two Catalan tuples, composed by $\circ$, yield $(e_0, \ldots, e_k)$. This implies that the number c_k of Catalan tuples in $\mathcal{C}_k$ satisfies Segner's recurrence relation

$$c_k = \sum_{m=0}^{k-1} c_m c_{k-1-m}$$

together with $c_0 = 1$, which is solved by the Catalan numbers $c_k = \frac{1}{k+1}\binom{2k}{k}$.

In Remark A.3 we formulate the $\circ$-decomposition in terms of Dyck paths.

The other composition of Catalan tuples is a variant of the $\circ$-product.

Definition 3.5 ($\bullet$-composition). The composition $\bullet\colon \mathcal{C}_k \times \mathcal{C}_l \to \mathcal{C}_{k+l+1}$ is given by

$$(e_0, \ldots, e_k) \bullet (f_0, \ldots, f_l) = (e_0 + 1, f_0, \ldots, f_l, e_1, \ldots, e_k).$$

As in the case of the composition $\circ$, Definition 3.4, no information is lost in the product $\bullet$. It is reverted by

$$\tilde{e} = (e_0, \dots, e_k) = (e_0 - 1, e_{1+\sigma_{e_0-1}(\tilde{e})}, \dots, e_k) \bullet (e_1, \dots, e_{\sigma_{e_0-1}(\tilde{e})}). \tag{11}$$

Because $\sigma_{e_0-1}(\tilde{e})$ exists for any $\tilde{e} \in \mathcal{C}_k$ with $k \geq 1$ (also for $e_0 = 1$, where one has $\sigma_{e_0-1}(\tilde{e}) = k$), every Catalan tuple has a unique pair of $\bullet$-factors. In Remark A.4 we formulate the $\bullet$-decomposition in terms of Dyck paths.

Out of these Catalan tuples we will construct three sorts of trees: *pocket tree*, *direct tree*, *opposite tree*. They are all planted plane trees, which means they are embedded into the plane and planted into a monovalent phantom root which connects to a unique vertex that we consider as the (real) root. We adopt the convention that the phantom root is not shown; its implicit presence manifests in a different counting of the valencies of the real root. Pocket tree and direct tree are the same, but their rôle will be different. Their drawing algorithms are given by the next definitions.

Definition 3.6 (direct tree, pocket tree). For a Catalan tuple $(e_0, \dots, e_k) \in \mathcal{C}_k$, draw $k+1$ vertices on a line. Starting at the root $l = 0$:

- unless $l = 0$, connect this vertex to the last vertex ($m < l$) with an open half-edge;
- if $e_l > 0$: e_l half-edges must be attached to vertex l;
- move to the next vertex.

For direct trees, vertices will be called *nodes* and edges will be called *threads*; they are oriented from left to right. For pocket trees, vertices are called *pockets*.

Definition 3.7 (opposite tree). For a Catalan tuple $(e_0, \dots, e_k) \in \mathcal{C}_k$, draw $k+1$ vertices on a line. Starting at the root $l = 0$:

- if $e_l > 0$: e_l half-edges must be attached to vertex l;
- if $e_l = 0$:
  - connect vertex l to the last vertex ($m < l$) with an open half-edge;
  - if vertex l is now not connected to the last vertex ($n \leq m < l$) with an open half-edge, repeat this until it is;
- move to the next vertex.

For opposite trees, vertices will be called *nodes* and edges will be called *threads*; they are oriented from left to right.

Examples of these trees can be seen in Figure 1 and Table 1. It will be explained in Section 5 how these trees relate to the recurrence relation (3) and how to label the nodes. The pocket trees will often be represented with a top-down orientation, instead of a left-right one.

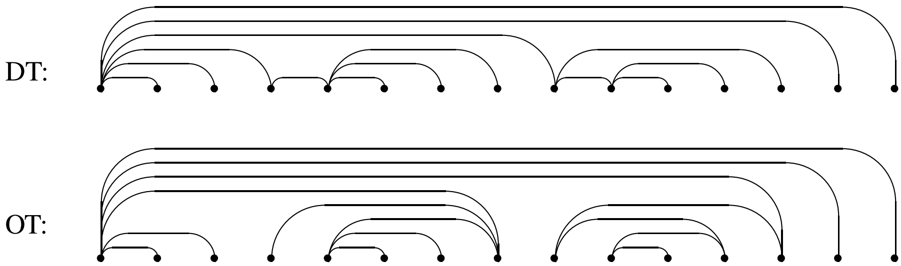

Figure 1. Direct tree (upper) and the opposite tree (lower) for the Catalan tuple (6, 0, 0, 1, 3, 0, 0, 0, 2, 2, 0, 0, 0, 0, 0) $=$ (5, 0, 0, 1, 3, 0, 0, 0, 2, 2, 0, 0, 0, 0) $\circ$ (0) $=$ $(5, 0, 1, 3, 0, 0, 0, 2, 2, 0, 0, 0, 0, 0) \bullet (0)$.

Catalan tuple	pocket tree	direct tree	opposite tree	Dyck path
(3,0,0,0)	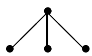	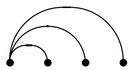	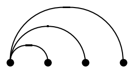	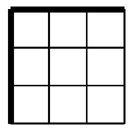
(2,1,0,0)	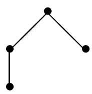	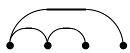	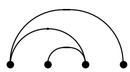	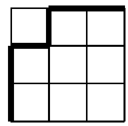
(2,0,1,0)	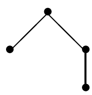	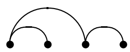	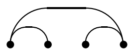	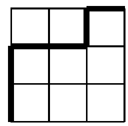
(1,2,0,0)	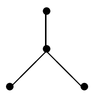	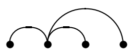	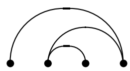	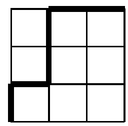
(1,1,1,0)			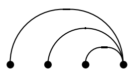	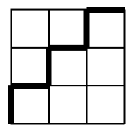

Table 1. Catalan tuples, their corresponding planted plane trees and Dyck paths for $k = 3$. The phantom roots of the planted plane trees are not shown. The real root is on top for the pocket tree and on the left for direct and opposite trees.

4. Nested Catalan tables

A nested Catalan table is a "Catalan tuple of Catalan tuples":

Definition 4.1 (nested Catalan table). A *nested Catalan table of length k* is a tuple

$$T_k = \langle \tilde{e}^{(0)}, \tilde{e}^{(1)}, \dots, \tilde{e}^{(k)} \rangle$$

of Catalan tuples $\tilde{e}^{(j)}$, such that $(1 + |\tilde{e}^{(0)}|, |\tilde{e}^{(1)}|, \dots, |\tilde{e}^{(k)}|)$, the *length* tuple of T_k, is itself a Catalan tuple of length k. We let $\mathcal{T}_k$ be the set of all nested Catalan tables of length k. The constituent $\tilde{e}^{(j)}$ in a nested Catalan table is called the j-th pocket.

We will show in Section 5 that a nested Catalan table contains all information about individual terms in the expansion (4) of the N-point function $G^{(0)}_{b_0 \dots b_{N-1}}$. Nested Catalan tables have a graphical presentation as diagrams of non-crossing chords with threads which we introduce in Appendix B.

Recall the composition $\circ$ from Definition 3.4 and the fact that any Catalan tuple of length ≥ 1 has a unique pair of $\circ$-factors. We extend $\circ$ as follows to nested Catalan tables:

Definition 4.2 ($\diamond$-operation). The operation $\diamond\colon \mathcal{T}_k \times \mathcal{T}_l \to \mathcal{T}_{k+l}$ is given by

$$\langle \tilde{e}^{(0)}, \dots, \tilde{e}^{(k)} \rangle \diamond \langle \tilde{f}^{(0)}, \dots, \tilde{f}^{(l)} \rangle := \langle \tilde{e}^{(0)} \circ \tilde{f}^{(0)}, \tilde{e}^{(1)}, \dots, \tilde{e}^{(k)}, \tilde{f}^{(1)}, \dots, \tilde{f}^{(l)} \rangle.$$

Now, suppose the nested Catalan table on the right-hand side is given. If the 0^{th} pocket has length ≥ 1, then it uniquely factors into $\tilde{e}^{(0)} \circ \tilde{f}^{(0)}$. Consider

$$\hat{k} = \sigma_{1+|\tilde{f}^{(0)}|}\big((1 + |\tilde{e}^{(0)} \circ \tilde{f}^{(0)}|, |\tilde{e}^{(1)}|, \dots, |\tilde{e}^{(k)}|, |\tilde{f}^{(1)}|, \dots, |\tilde{f}^{(l)}|)\big). \tag{12}$$

By construction, $\hat{k} = k$ so that $\diamond$ can be uniquely reverted. Note also that nested Catalan tables $\langle (0), \tilde{e}_1, \dots, \tilde{e}_k \rangle$ do not have a $\diamond$-decomposition.

The composition $\bullet$ of Catalan tuples is extended as follows to nested Catalan tables:

Definition 4.3 ($\blacklozenge$-operation). The operation $\blacklozenge\colon \mathcal{T}_k \times \mathcal{T}_l \to \mathcal{T}_{k+l}$ is given by

$$\langle \tilde{e}^{(0)}, \dots, \tilde{e}^{(k)} \rangle \blacklozenge \langle \tilde{f}^{(0)}, \dots, \tilde{f}^{(l)} \rangle := \langle \tilde{e}^{(0)}, \tilde{e}^{(1)} \bullet \tilde{f}^{(0)}, \tilde{f}^{(1)}, \dots, \tilde{f}^{(l)}, \tilde{e}^{(2)}, \dots, \tilde{e}^{(k)} \rangle.$$

If the 1^{st} pocket has length ≥ 1, it uniquely factors as $\tilde{e}^{(1)} \bullet \tilde{f}^{(0)}$, and we extract

$$\hat{l} := \sigma_{|\tilde{e}^{(0)}|+|\tilde{e}^{(1)}|+1}\big((1 + |\tilde{e}^{(0)}|, |\tilde{e}^{(1)} \bullet \tilde{f}^{(0)}|, |\tilde{f}^{(1)}|, \dots, |\tilde{f}^{(l)}|, |\tilde{e}^{(2)}|, \dots, |\tilde{e}^{(k)}|)\big). \tag{13}$$

By construction $\hat{l} = l$, and $\blacklozenge$ is uniquely reverted.

We let $\mathcal{S}_k = \{\langle \tilde{e}_0, (0), \tilde{e}_2, \dots, \tilde{e}_k \rangle \in \mathcal{T}_k\}$ be the subset of length-k nested Catalan tables having (0) as their 1^{st} pocket. The nested Catalan tables $S \in \mathcal{S}_k$ are precisely those which do not have a $\blacklozenge$-decomposition. The distinction between $\mathcal{S}_l$ and its complement in $\mathcal{T}_l$ is the key to determine the number of nested Catalan tables:

Proposition 4.4. *The set $\mathcal{T}_{k+1}$ of nested Catalan tables and its subset $\mathcal{S}_{k+1}$ with* 1^{st} *pocket* (0) *have cardinalities*

$$d_k := |\mathcal{T}_{k+1}| = \frac{1}{k+1}\binom{3k+1}{k} \quad \textit{and} \quad h_k := |\mathcal{S}_{k+1}| = \frac{1}{2k+1}\binom{3k}{k}. \tag{14}$$

Proof. Let

$$\mathcal{D}(x) := \sum_{k=1}^{\infty} x^k \sum_{T\in\mathcal{T}_k} T \quad \text{and} \quad \mathcal{H}(x) := \sum_{k=1}^{\infty} x^k \sum_{S\in\mathcal{S}_k} S$$

be the generating function of the set of all nested Catalan tables and of those having (0) as their 1^{st} pocket, respectively. Then

$$\mathcal{D}(x) = \mathcal{D}(x)\blacklozenge\mathcal{D}(x) + \mathcal{H}(x) \tag{15}$$

because precisely the complements $\mathcal{T}_k \setminus \mathcal{S}_k$ have a unique $\blacklozenge$-decomposition. With the exception of $\langle(0),(0)\rangle \in \mathcal{S}_1 = \mathcal{T}_1$, all $S = \langle\tilde{e}^0,(0),\tilde{e}^2,\dots,\tilde{e}^k\rangle \in \mathcal{S}_k$ with $k \geq 2$ have $|\tilde{e}^0| \geq 1$. Therefore, they have a unique $\lozenge$-decomposition, where the left factor necessarily belongs to $\mathcal{S}_l$ for some l:

$$\mathcal{H}(x) = \mathcal{H}(x)\lozenge\mathcal{D}(x) + x\langle(0),(0)\rangle. \tag{16}$$

Introducing the generating functions

$$D(x) = \sum_{k=0}^{\infty} x^{k+1} d_k \quad \text{and} \quad H(x) = \sum_{k=0}^{\infty} x^{k+1} h_k$$

of the cardinalities $d_k = |\mathcal{T}_{k+1}|$ and $h_k = |\mathcal{S}_{k+1}|$, equations (15) and (16) project to quadratic relations

$$D(x) = D(x)\cdot D(x) + H(x) \quad \text{and} \quad H(x) = H(x)\cdot D(x) + x. \tag{17}$$

Multiplying the first equation by $H(x)$ and the second one by $D(x)$ gives $x \cdot D(x) = H^2(x)$, which separates (17) into cubic relations

$$D(x)(1-D(x))^2 = x \quad \text{and} \quad \frac{H(x)}{\sqrt{x}}\Big(1-\Big(\frac{H(x)}{\sqrt{x}}\Big)^2\Big) = \sqrt{x}. \tag{18}$$

The assertion (14) follows from the Lagrange inversion formula.[1] To obtain the first equation (14) one sets $f(x) = x(1-x)^2$ and $\phi(x) = \frac{1}{(1-x)^2}$ to get

$$d_k = \frac{1}{k+1}[x^k]\frac{1}{(1-x)^{2k+2}}.$$

To obtain the second equation (14) one sets $\sqrt{x} = y$, $f(y) = y(1-y^2)$ and $\phi(y) = \frac{1}{1-y^2}$ to get $h_k = \frac{1}{2k+1}[y^{2k}]\frac{1}{(1-y^2)^{2k+1}} = \frac{1}{2k+1}[x^k]\frac{1}{(1-x)^{2k+1}}$. ■

Remark 4.5. More information about the integer sequences d_k (A006013) and h_k (A001764) can be found via [16] and [15], respectively. Equations (18) are higher-order variants of the equation $C(x)(1-C(x)) = x$ for the generating function $C(x) = \sum_{n=0}^{\infty} c_n x^{n+1}$ of Catalan numbers.

Corollary 4.6. *The number d_k of nested Catalan tables satisfies*

$$d_k = \sum_{(e_0,\dots,e_{k+1})\in\mathcal{C}_{k+1}} c_{e_0-1}c_{e_1}\cdots c_{e_k}c_{e_{k+1}}. \tag{19}$$

Proof. There are $c_{|\tilde{e}_0|}\cdots c_{|\tilde{e}_{k+1}|}$ nested Catalan tables $\langle\tilde{e}_0,\dots,\tilde{e}_{k+1}\rangle$ of the same length tuple $(|\tilde{e}_0|+1, |\tilde{e}_1|,\dots,|\tilde{e}_{k+1}|) \in \mathcal{C}_{k+1}$. Set $e_0 = |\tilde{e}_0|+1$ and $e_j = |\tilde{e}_j|$ for $j = 1,\dots,k+1$. ■

5. The bijection between nested Catalan tables and contributions to $G^{(0)}_{b_0\dots b_{N-1}}$

This section is the main part of this paper. We will omit in the sequel the superscript $G^{(0)}_{b_1b_2} = G_{b_1b_2}$. We remark that the graphical presentation given in Appendix B was very helpful to identify this bijection.

Definition 5.1. To a nested Catalan table $T_{k+1} = \langle\tilde{e}^{(0)},\tilde{e}^{(1)},\dots,\tilde{e}^{(k+1)}\rangle \in \mathcal{T}_{k+1}$ with $N/2 = k+1$ we associate a monomial $[T]_{b_0,\dots,b_{N-1}}$ in $G_{b_lb_m}$ and $\frac{1}{E_{b_{l'}}-E_{b_{m'}}}$ as follows.

(1) Build the pocket tree for the length tuple $(1+|\tilde{e}^{(0)}|, |\tilde{e}^{(1)}|,\dots,|\tilde{e}^{(k+1)}|) \in \mathcal{C}_{k+1}$. It has $k+1$ edges and every edge has two sides. Starting from the root and

[1] *Lagrange inversion formula.* Let $f, g \in x\mathbb{C}[[x]]$ be formal power series inverse to each other, $g(f(x)) = x$. Then their coefficients are related by $[x^n]g(x) = \frac{1}{n}[x^{-1}]\frac{1}{(f(x))^n}$. In particular, for $f(x) = \frac{x}{\phi(x)}$ one has $[x^n]g(x) = \frac{1}{n}[x^{n-1}](\phi(x))^n$.

turning counterclockwise, label the edge sides in consecutive order[2] from b_0 to b_{N-1}. An edge labelled $b_l b_m$ encodes a factor $G_{b_l b_m}$ in $G^{(0)}_{b_0 \dots b_{N-1}}$.

(2) Label the $k+2$ vertices of the pocket tree by $P_0, \dots, P_{k+1}$ in consecutive order[2] when turning counterclockwise around the tree. Let $v(P_m)$ be the valency of vertex P_m (number of edges attached to P_m) and L_m be the distance between P_m and the root P_0 (number of edges in shortest path between P_m and P_0).

(3) For every vertex P_m that is not a leaf, read off the $2v(P_m)$ side labels of edges connected to P_m. Draw two rows of $v(P_m)$ nodes each. Label the nodes of the first row by the even edge side labels in natural order, i.e., starting at the edge closest to the root and proceed in the counterclockwise direction. Label the nodes of the other row by the odd edge side labels using the same edge order. Take the m-th Catalan tuple $\tilde{e}^{(m)}$ of the nested Catalan table. If L_m is even, draw the direct (resp. opposite) tree encoded by $\tilde{e}^{(m)}$ between the row of even (resp. odd) nodes. If L_m is odd, draw the opposite (resp. direct) tree encoded by $\tilde{e}^{(m)}$ between the row of even (resp. odd) nodes. Encode a thread from b_l to b_m in the direct or opposite tree by a factor $\frac{1}{E_{b_l} - E_{b_m}}$.

Remark 5.2. In proofs below we sometimes have to insist that one side label of a pocket edge is a particular b_k, whereas the label of the other side does not matter. Is such a situation we will label the other side by $b_{\bar{k}}$. Note that if b_k is even (resp. odd), then $b_{\bar{k}}$ is odd (resp. even).

Remark 5.3. For the purpose of this article it is sufficient to mention that an explicit construction for the level function $L_m \colon \mathcal{C}_{k+1} \to \{0, \dots, k\}$ exists.

Example 5.4. Let $T = \langle (2,0,0), (1,1,0), (0), (0), (0), (1,0), (0) \rangle \in \mathcal{T}_6$. Its length tuple is $(3,2,0,0,0,1,0) \in \mathcal{C}_6$, which defines the pocket tree:

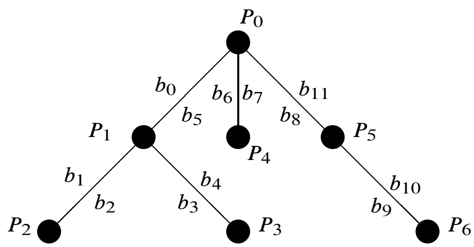

The edge side labels encode

$$G_{b_0 b_5} G_{b_1 b_2} G_{b_3 b_4} G_{b_6 b_7} G_{b_8 b_{11}} G_{b_9 b_{10}}.$$

[2]This is the same order as in [14, Figure 5.14].

For vertex P_0, at even distance, we draw direct and opposite tree encoded in $\tilde{e}^{(0)} = (2, 0, 0)$:

For vertex P_1, at odd distance, we draw opposite and direct tree encoded in $\tilde{e}^{(1)} = (1, 1, 0)$:

For vertex P_5, at odd distance, we draw opposite and direct tree encoded in $\tilde{e}^{(5)} = (1, 0)$:

They give rise to a factor

$$\frac{1}{(E_{b_0} - E_{b_6})(E_{b_0} - E_{b_8})(E_{b_0} - E_{b_4})(E_{b_2} - E_{b_4})(E_{b_8} - E_{b_{10}})} \\ \times \frac{1}{(E_{b_5} - E_{b_7})(E_{b_5} - E_{b_{11}})(E_{b_5} - E_{b_1})(E_{b_1} - E_{b_3})(E_{b_{11}} - E_{b_9})}.$$

Later in Figure 4 we give a diagrammatic representation of this nested Catalan table.

The following theorem shows that the nested Catalan tables correspond bijectively to the terms in the expansion of the recurrence relation (3).

Theorem 5.5. *The recurrence* (3) *of N-point functions in the quartic matrix model* (1) *has the explicit solution*

$$G^{(0)}_{b_0 \ldots b_{N-1}} = \sum_{T \in \mathcal{T}_{k+1}} [T]_{b_0 \ldots b_{N-1}},$$

where the sum is over all nested Catalan tables of length $N/2 = k + 1$ and the monomials $[T]_{b_0 \ldots b_{N-1}}$ are described in Definition 5.1.

Proof. We proceed by induction in N. For $N = 2$ the only term in the 2-point function corresponds to the nested Catalan table $\langle (0), (0) \rangle \in \mathcal{T}_1$. Its associated length tuple $(1, 0)$ encodes the pocket tree

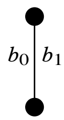

whose single edge corresponds to a factor $G_{b_0 b_1}$. The Catalan tuples of both pockets have length 0, so that there is no denominator.

For any contribution to $G^{(0)}_{b_0\dots b_{N-1}}$ with $N \geq 4$, encoded by a length-$N/2$ nested Catalan table $T_{N/2}$, it must be shown that $T_{N/2}$ splits in one or two ways into smaller nested Catalan tables whose corresponding monomials produce $T_{N/2}$ via (3). There are three cases to consider.

Case I: $T_{k+1} = \langle (0), \tilde{e}^{(1)}, \dots, \tilde{e}^{(k+1)} \rangle \in \mathcal{T}_{k+1}$ with $N/2 = k+1$. It follows from Definition 4.3 that there are uniquely defined nested Catalan tables $T_l = \langle \tilde{f}, \tilde{e}^{(2)}, \dots, \tilde{e}^{(l+1)} \rangle \in \mathcal{T}_l$ and $T_{k-l+1} = \langle (0), \tilde{e}, \tilde{e}^{(l+2)}, \dots, \tilde{e}^{(k+1)} \rangle \in \mathcal{T}_{k-l+1}$ with $\tilde{e}^{(1)} = \tilde{e} \bullet \tilde{f}$ and consequently $T_{k-l+1} \blacklozenge T_l = T_{k+1}$. The length $l = \hat{l}$ is obtained via (13). Recall that T_{k+1} cannot be obtained by the $\diamond$-composition because the zeroth pocket has length $|(0)| = 0$. By induction, T_l encodes a unique contribution $[T_l]_{b_1\dots b_{2l}}$ to $G^{(0)}_{b_1\dots b_{2l}}$, and T_{k-l+1} encodes a unique contribution $[T_{k-l+1}]_{b_0 b_{2l+1}\dots b_{N-1}}$ to $G^{(0)}_{b_0 b_{2l+1}\dots b_{N-1}}$. We have to show that

$$-\frac{[T_l]_{b_1\dots b_{2l}} [T_{k-l+1}]_{b_0 b_{2l+1}\dots b_{N-1}}}{(E_{b_0} - E_{b_{2l}})(E_{b_1} - E_{b_{N-1}})}$$

agrees with $[T_{k+1}]_{b_0\dots b_{N-1}}$ encoded by T_{k+1}. A detail of the pocket tree of T_{k+1} sketching P_0, P_1 and their attached edges is

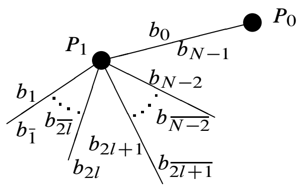

(20)

Only the gluing of the direct and opposite tree encoded by $\tilde{e} = (e_0, \dots, e_p)$ with the direct and opposite tree encoded by $\tilde{f} = (f_0, \dots, f_q)$ via a thread from b_0 to b_{2l} and a thread from b_{N-1} to b_1 remains to be shown; edge sides encoding $G^{(0)}_{b_k b_l}$ and all other pockets are automatic. A symbolic notation is used now to sketch the trees. Horizontal dots are used to indicate a general direct tree and horizontal dots with vertical dots above them indicate an opposite tree. Unspecified threads are indicated by dotted half-edges. The four trees mentioned above are depicted as

$\mathrm{OT}_{\tilde{e}} =$ 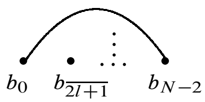

$\mathrm{OT}_{\tilde{f}} =$ 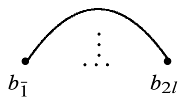

$\mathrm{DT}_{\tilde{e}} =$ 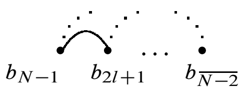

$\mathrm{DT}_{\tilde{f}} =$ 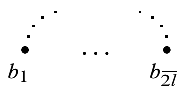

Here $\tilde{e}$ describes P_1, at odd distance, so that even-labelled nodes are connected by the opposite tree. Every edge in the pocket tree has two sides labelled b_r and b_s, where the convention of Remark 5.2 is used when the other side label does not matter.

The first edge in the pocket tree has side labels $b_0 b_{N-1}$ and descends from the root pocket. The following edge is $b_{\overline{2l+1}} b_{2l+1}$ where $2l+2 \leq \overline{2l+1} \leq N-2$ is an even number. The final edge is $b_{N-2} b_{\overline{N-2}}$ where $2l+1 \leq \overline{N-2} \leq N-3$ is an odd number.

Next, $\tilde{f}$ encodes P_0 in the pocket tree belonging to $[T_l]_{b_1 \dots b_{2l}}$. It lies at even distance, but, because the labels at $G^{(0)}_{b_1 \dots b_{2l}}$ start with an odd one, the odd nodes of $\tilde{f}$ are connected by the direct tree and the even nodes by the opposite tree. Again, $2 \leq \overline{1} \leq 2l$ denotes an even number and $1 \leq \overline{2l} \leq 2l-1$ an odd number. When pasting $\tilde{f}$ into $\tilde{e}$, the first edge remains $b_0 b_{N-1}$, which descends from the root. Then all edges from $\tilde{f}$ follow and, finally, the remaining edges of $\tilde{e}$. Thus, before taking the denominators into account, the four trees are arranged as

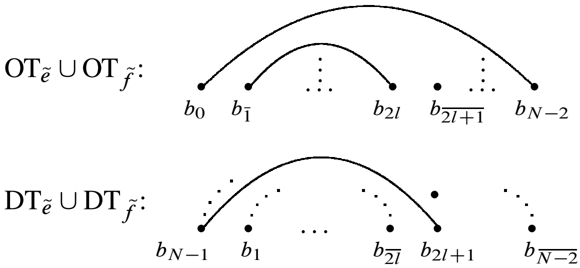

(21)

The denominator of $\frac{1}{(E_{b_0}-E_{b_{2l}})(E_{b_{N-1}}-E_{b_1})}$ (with rearranged sign) corresponds to a thread between the nodes b_0 and b_{2l} and one between the nodes b_{N-1} and b_1:

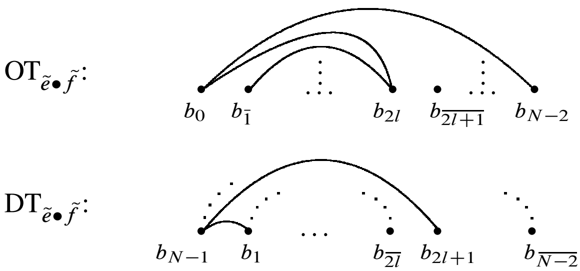

(22)

The result is precisely described by $\tilde{e} \bullet \tilde{f} = (e_0+1, f_0, \dots, f_q, e_1, \dots, e_p)$ with Definitions 3.6 and 3.7. Indeed, the increased zeroth entry corresponds to one additional half-thread attached to the first node b_{N-1} and one additional half-thread to b_0. For the direct tree the rules imply that the next node, b_1, is connected to b_{N-1}. This is the new thread from the denominators. The next operations are done within $\tilde{f}$, labelled $b_1, \dots, b_{\overline{2l}}$, without any change. Arriving at its final node $b_{\overline{2l}}$ all half-threads of $\tilde{f}$ are connected. The next node, labelled b_{2l+1}, connects to the previous open half-thread, which is the very first node b_{N-1}. These and all the following connections arise within $\tilde{e}$ and remain unchanged. Similarly, in the opposite tree, we first open e_0+1 half-threads at the zeroth node b_0. Since $f_0>0$, we subsequently open f_0 half-threads at the first node $b_{\bar{1}}$. The next operations remain unchanged, until we arrive at the final node b_{2l} of $\tilde{f}$. It corresponds to $f_q=0$, so that we connect it to all previous open half-threads, first within $\tilde{f}$. However, because $e_0+1>0$, it is connected by an additional thread to b_0 and encodes the denominator of $\frac{1}{E_{b_0}-E_{b_{2l}}}$. This consumes the additional half-thread attached to b_0. All further connections are the same as within $\tilde{e}$. In conclusion, we obtain precisely the nested Catalan table $T_{k+1}=\langle(0),\tilde{e}^{(1)},\dots,\tilde{e}^{(N/2)}\rangle$ we started with.

Case II: $\boldsymbol{T_{k+1}=\langle\tilde{e}^{(0)},(0),\tilde{e}^{(2)},\dots,\tilde{e}^{(k+1)}\rangle\in\mathcal{T}_{k+1}}$ and $\boldsymbol{N/2=k+1}$. There are uniquely defined nested Catalan tables $T_l=\langle\tilde{e},(0),\tilde{e}^{(2)},\dots,\tilde{e}^{(l)}\rangle\in\mathcal{T}_l$ and $T_{k-l+1}=\langle\tilde{f},\tilde{e}^{(l+1)},\dots,\tilde{e}^{(k+1)}\rangle\in\mathcal{T}_{k-l+1}$ with $\tilde{e}^{(0)}=\tilde{e}\circ\tilde{f}$ and, consequently, $T_l\diamond T_{k-l+1}=T_{k+1}$. The length $l=\hat{k}$ is obtained via (12). Recall that T_{k+1} cannot be obtained by the $\blacklozenge$-composition, because the 1st entry has length $|(0)|=0$. By the induction hypothesis, T_l encodes a unique contribution $[T_l]_{b_0\dots b_{2l-1}}$ to $G^{(0)}_{b_0\dots b_{2l-1}}$ and T_{k-l+1} encodes a unique contribution $[T_{k-l+1}]_{b_{2l}\dots b_{N-1}}$ to $G^{(0)}_{b_{2l}\dots b_{N-1}}$. It remains to be shown that

$$\frac{[T_l]_{b_0\dots b_{2l-1}}[T_{k-l+1}]_{b_{2l}\dots b_{N-1}}}{(E_{b_0}-E_{b_{2l}})(E_{b_1}-E_{b_{N-1}})}$$

agrees with $[T_{k+1}]_{b_0\dots b_{N-1}}$ encoded by T_{k+1}. A detail of the pocket tree of T_{k+1} sketching P_0, P_1 and their attached edges is

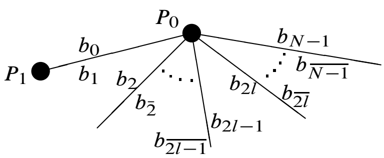

(23)

As in Case I, only the gluing of the direct and opposite tree encoded by $\tilde{e}=(e_0,\dots,e_p)$ with the direct and opposite tree encoded by $\tilde{f}=(f_0,\dots,f_q)$ via a thread from b_0 to b_{2l} and a thread from b_1 to b_{N-1} must be demonstrated. Everything else is automatic. These trees are

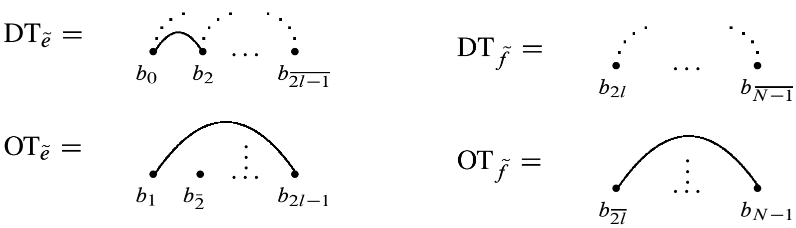

(24)

The notation is the same as in Case I. The 1st pocket P_1, described by the Catalan tuple (0), is only 1-valent so that the first edge is labelled b_0b_1. The direct trees in (24) are put next to each other and a thread between b_0 and b_{2l} is drawn for the denominator of $\frac{1}{E_{b_0}-E_{b_{2l}}}$. Similarly, the opposite trees in (24) are put next to each other and a thread between b_1 and b_{N-1} is drawn for the denominator of $\frac{1}{E_{b_1}-E_{b_{N-1}}}$:

$\mathrm{DT}_{\tilde{e}\circ\tilde{f}} =$

$\mathrm{OT}_{\tilde{e}\circ\tilde{f}} =$

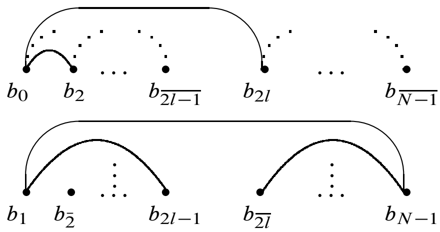

The result are precisely the direct and opposite trees of the composition

$$\tilde{e}\circ\tilde{f} = (e_0+1, e_1, \ldots, e_p, f_0, \ldots, f_q).$$

The increase $e_0 \to e_0+1$ opens an additional half-thread at b_0 and an additional half-thread at b_1. In the direct tree, this new half-thread is not used by $e_1, \ldots, e_p$. Only when we are moving to f_0, labelled b_{2l}, we have to connect it with the last open half-thread, i.e., with b_0. After that the remaining operations are unchanged compared with $\tilde{f}$. In the opposite tree, the additional half-thread at b_1 is not used in $e_1, \ldots, e_p$. Because f_0, labelled $b_{\overline{2l}}$, opens enough half-threads, it is not consumed by $f_0, \ldots, f_{q-1}$ either. Then, the last node f_q, labelled b_{N-1}, successively connects to all nodes with open half-threads, including b_1. In conclusion, we obtain precisely the nested Catalan table $T_{k+1} = \langle \tilde{e}^{(0)}, (0), \tilde{e}^{(2)}, \ldots, \tilde{e}^{(N/2)}\rangle$ we started with.

Case III: we consider a general $T_{k+1} = \langle \tilde{e}^{(0)}, \tilde{e}^{(1)}, \tilde{e}^{(2)}, \ldots, \tilde{e}^{(k+1)}\rangle \in \mathcal{T}_{k+1}$ with $k+1 = N/2$, $|\tilde{e}^{(0)}| \geq 1$ and $|\tilde{e}^{(1)}| \geq 1$. There are uniquely defined nested Catalan tables

$$T_l = \langle \tilde{e}, \tilde{e}^{(1)}, \tilde{e}^{(2)}, \ldots, \tilde{e}^{(l)}\rangle \in \mathcal{T}_l$$

and

$$T_{k-l+1} = \langle \tilde{f}, \tilde{e}^{(l+1)}, \ldots, \tilde{e}^{(k+1)}\rangle \in \mathcal{T}_{k-l+1}$$

with $\tilde{e}^{(0)} = \tilde{e}\circ\tilde{f}$ and consequently

$$T_l \diamond T_{k-l+1} = T_{k+1}.$$

Moreover, there exist uniquely defined nested Catalan tables

$$T_{l'} = \langle \tilde{f}', \tilde{e}^{(2)}, \ldots, \tilde{e}^{(l'+1)}\rangle \in \mathcal{T}_{l'}$$

and

$$T_{k-l'+1} = \langle \tilde{e}^{(0)}, \tilde{e}', \tilde{e}^{(l'+2)}, \dots, \tilde{e}^{(k+1)} \rangle \in \mathcal{T}_{k-l'+1}$$

such that $\tilde{e}^{(1)} = \tilde{e}' \bullet \tilde{f}'$ and consequently

$$T_{k-l'+1} \blacklozenge T_{l'} = T_{k+1}.$$

We necessarily have $l' \leq k-1$ and $l \geq 2$, because $l' = k$ corresponds to Case I and $l = 1$ to Case II. By the induction hypothesis, these nested Catalan subtables encode unique contributions $[T_l]_{b_0 \dots b_{2l-1}}$ to $G^{(0)}_{b_0 \dots b_{2l-1}}$, $[T_{k-l+1}]_{b_{2l} \dots b_{N-1}}$ to $G^{(0)}_{b_{2l} \dots b_{N-1}}$, $[T_{l'}]_{b_1 \dots b_{2l'}}$ to $G^{(0)}_{b_1 \dots b_{2l'}}$ and $[T_{k-l'+1}]_{b_0 b_{2l'+1} \dots b_{N-1}}$ to $G^{(0)}_{b_0 b_{2l'+1} \dots b_{N-1}}$. We have to show that

$$\frac{[T_l]_{b_0 \dots b_{2l-1}} [T_{N/2-l}]_{b_{2l} \dots b_{N-1}}}{(E_{b_0} - E_{b_{2l}})(E_{b_1} - E_{b_{N-1}})} - \frac{[T_{l'}]_{b_1 \dots b_{2l'}} [T_{N/2-l'}]_{b_0 b_{2l'+1} \dots b_{N-1}}}{(E_{b_0} - E_{b_{2l'}})(E_{b_1} - E_{b_{N-1}})} \tag{25}$$

agrees with $[T_{k+1}]_{b_0 \dots, b_{N-1}}$.

In the pocket tree of T_{k+1} there must be an edge with side labels $b_0 b_h$, where $3 \leq h \leq N-3$ and h is odd. Here is a detail of the pocket tree of T_{k+1} showing P_0, P_1:

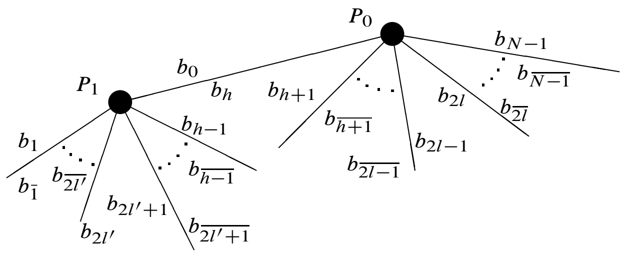

(26)

The direct and opposite trees for $\tilde{e}$, $\tilde{f}$ and $\tilde{e}^{(1)}$ can be sketched as

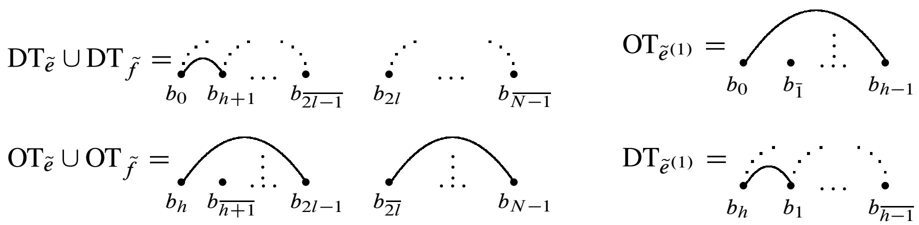

(27)

The denominators of $\frac{1}{(E_{b_0}-E_{b_{2l}})(E_{b_1}-E_{b_{N-1}})}$ in (25) add threads from b_0 to b_{2l} and from b_1 to b_{N-1}. The first one connects the direct trees for $\tilde{e} \cup \tilde{f}$ to the direct tree encoded by $\tilde{e}^{(0)} = \tilde{e} \circ \tilde{f}$. The second thread does *not* give a valid composition of the opposite trees for $\tilde{e} \cup \tilde{f}$.

This is a problem. The solution is to split this contribution. Half of the contribution is sacrificed to bring the other half in the desired form. Afterwards, the same procedure is repeated for the other term in (25) with a minus-sign. The remainders are the same and cancel each other, whereas the other halves add up to yield the sought for monomial.

Returning to trees, we note that in the direct tree for the pocket $\tilde{e}^{(1)}$ there is always a thread from b_h to b_1, encoding a factor $\frac{1}{E_{b_h}-E_{b_1}}$. With the factor $\frac{1}{E_{b_1}-E_{b_{N-1}}}$ it fulfils

$$\frac{1}{E_{b_h}-E_{b_1}}\cdot\frac{1}{E_{b_1}-E_{b_{N-1}}}=\frac{1}{E_{b_h}-E_{b_1}}\cdot\frac{1}{E_{b_h}-E_{b_{N-1}}}+\frac{1}{E_{b_h}-E_{b_{N-1}}}\cdot\frac{1}{E_{b_1}-E_{b_{N-1}}}. \tag{28}$$

The first term on the right-hand side of (28) leaves the direct tree $\mathrm{DT}_{\tilde{e}^{(1)}}$ as it is and connects the parts of $\mathrm{OT}_{\tilde{e}}\cup\mathrm{OT}_{\tilde{f}}$ via the thread from b_h to b_{N-1} to form $\mathrm{OT}_{\tilde{e}^{(0)}}$, where $\tilde{e}^{(0)}=\tilde{e}\circ\tilde{f}$.

The final term in (28) also unites $\mathrm{OT}_{\tilde{e}}\cup\mathrm{OT}_{\tilde{f}}$ and forms $\mathrm{OT}_{\tilde{e}^{(0)}}$, but it removes in $\mathrm{DT}_{\tilde{e}^{(1)}}$ the thread between b_h and b_1. It follows from $\tilde{e}^{(1)}=\tilde{e}'\bullet\tilde{f}'$ that this tree falls apart into the subtrees $\mathrm{DT}_{\tilde{e}'}$, containing b_h, and $\mathrm{DT}_{\tilde{f}'}$, which contains b_1. These are multiplied by a factor $\frac{1}{E_{b_1}-E_{b_{N-1}}}$. The second term in (25) will remove them.

Indeed, direct and opposite trees for $\tilde{e}^{(0)}$, $\tilde{e}'$ and $\tilde{f}'$ can be sketched as

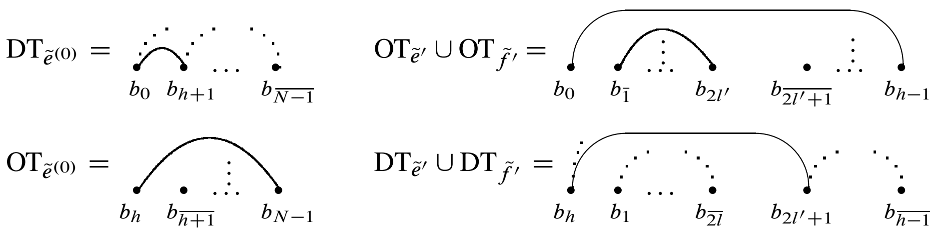

(29)

The direct tree $\mathrm{DT}_{\tilde{e}^{(0)}}$ remains intact and the thread from b_0 to $b_{2l'}$ encoded in the factor $\frac{1}{(E_{b_0}-E_{b_{2l'}})}$ in (25) connects the opposite trees for $\tilde{e}'\cup\tilde{f}'$ to form the opposite tree for $\tilde{e}^{(1)}=\tilde{e}'\bullet\tilde{f}'$. The direct trees $\mathrm{DT}_{\tilde{e}'}\cup\mathrm{DT}_{\tilde{f}'}$ remain disconnected and are multiplied by $\frac{1}{(E_{b_1}-E_{b_{N-1}})}$ from (25). With the minus-sign from (25) they cancel the final term in (28). The other trees combined yield precisely the direct and opposite trees for both $\tilde{e}^{(0)}$ and $\tilde{e}^{(1)}$, so that the single nested Catalan table we started with is retrieved.

This completes the proof. Bijectivity between nested Catalan tables and contributing terms to $(N'<N)$-point functions is essential: Assuming the above construction in Cases I–III missed nested Catalan subtables $T_l, T_{N/2-l}$, then their composition $T_l\diamond T_{N/2-l}$ would be a new nested Catalan table of length $N/2$. However, all nested Catalan tables of length $N/2$ are considered. Similarly, for $T_{l'}\blacklozenge T_{N/2-l'}$. ∎

This theorem shows that there is a one-to-one correspondence between nested Catalan tables and the diagrams/terms in $G^{(0)}_{b_0\ldots b_{N-1}}$ with designated node b_0. The choice of designated node does not influence $G^{(0)}_{b_0\ldots b_{N-1}}$, but it does alter its expansion.

A. Examples

Example A.1. We have $(1,0) = (0) \circ (0)$, $(2,0,0) = (1,0) \circ (0)$, $(1,1,0) = (0) \circ (1,0)$ and $(3,1,0,0,2,0,0) = (2,1,0,0) \circ (2,0,0)$.

Example A.2. We have $(1,0) = (0) \bullet (0)$, $(2,0,0) = (1,0) \bullet (0)$, $(1,1,0) = (0) \bullet (1,0)$ and $(3,1,0,0,2,0,0) = (2,0,2,0,0) \bullet (1,0)$.

Remark A.3. We formulate the $\circ$-decomposition in terms of Dyck paths.

(1) Remove the lowest row of the lattice.

(2) Draw the north-east diagonal from the new bottom-left corner. Let F be the first step east which goes below the north-east diagonal.

(3) Remove the column containing F.

(4) The left $\circ$-factor is the Dyck path in the lattice obtained by retaining only the rows and columns shared by the part of the north-east diagonal left of F.

(5) The right $\circ$-factor is the Dyck path in the lattice obtained by deleting (in addition to steps 1. and 3.) all rows and columns shared by the part of the north-east diagonal left of F.

If the resulting lattice in one of the factors is empty this corresponds to the Catalan tuple (0) of length 0. For example, the decomposition $(3,1,0,0,2,0,0) = (2,1,0,0) \circ (2,0,0)$ visualises as

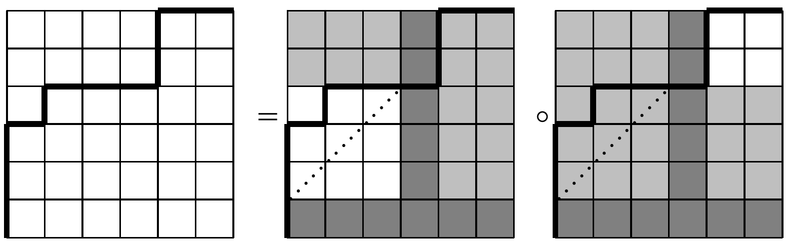

The row and column removed in steps 1. and 3. are shown in darker gray. The north-east diagonal is dotted.

Remark A.4. We formulate the $\bullet$-decomposition in terms of Dyck paths.

(1) Remove the lowest row of the lattice.

(2) Draw the north-east diagonal from the end point of the very first step east. Let F be the first step east which goes below this north-east diagonal.

(3) Remove the column containing F.

(4) The left $\bullet$-factor is the Dyck path in the lattice obtained by deleting (in addition to steps 1. and 3.) all rows and columns shared by the part of the north-east diagonal left of F.

(5) The right $\bullet$-factor is the Dyck path in the lattice obtained by retaining only the rows and columns shared by the part of the north-east diagonal left of F.

If the resulting lattice in one of the factors is empty this corresponds to the Catalan tuple (0) of length 0. For example, the decomposition

$$(3, 1, 0, 0, 2, 0, 0) = (2, 0, 2, 0, 0) \bullet (1, 0)$$

visualises as

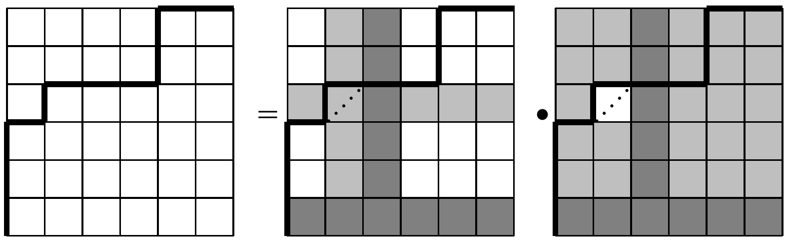

The row and column removed in steps 1. and 3. are shown in darker gray. The north-east diagonal is dotted.

Example A.5. We have

$$\begin{aligned}
\mathcal{T}_1 &= \{\langle(0), (0)\rangle\},\\
\mathcal{T}_2 &= \{\langle(1,0), (0), (0)\rangle,\ \langle(0), (1,0), (0)\rangle\},\\
\mathcal{T}_3 &= \{\langle(2,0,0), (0), (0), (0)\rangle,\ \langle(1,1,0), (0), (0), (0)\rangle,\ \langle(1,0), (1,0), (0), (0)\rangle,\\
&\qquad \langle(1,0), (0), (1,0), (0)\rangle,\ \langle(0), (2,0,0), (0), (0)\rangle,\ \langle(0), (1,1,0), (0), (0)\rangle,\\
&\qquad \langle(0), (1,0), (1,0), (0)\rangle\}.
\end{aligned}$$

Later in Figures 2 and 3 we give a diagrammatic representation of the nested Catalan tables in $\mathcal{T}_2$ and $\mathcal{T}_3$, respectively.

Example A.6. We have $\langle(2,0,0), (0), (0), (0)\rangle = \langle(1,0), (0), (0)\rangle \diamond \langle(0), (0)\rangle$ and $\langle(1,1,0), (0), (0), (0)\rangle = \langle(0), (0)\rangle \diamond \langle(1,0), (0), (0)\rangle$. In Example 5.4 and Figure 4 we considered the nested Catalan table $\langle(2,0,0), (1,1,0), (0), (0), (0), (1,0), (0)\rangle = \langle(1,0), (1,1,0), (0), (0), (0)\rangle \diamond \langle(0), (1,0), (0)\rangle$. Another example will be given in Example B.2.

Example A.7. We have $\langle(0),(2,0,0),(0),(0)\rangle = \langle(0),(1,0),(0)\rangle\blacklozenge\langle(0),(0)\rangle$ and $\langle(0),(1,1,0),(0),(0)\rangle = \langle(0),(0)\rangle\blacklozenge\langle(1,0),(0),(0)\rangle$. In Example 5.4 and Figure 4 we considered the nested Catalan table $\langle(2,0,0),(1,1,0),(0),(0),(0),(1,0),(0)\rangle = \langle(2,0,0),(0),(0),(1,0),(0)\rangle\blacklozenge\langle(1,0),(0),(0)\rangle$. Another example will be given in Example B.3.

B. Chord diagrams with threads

For uncovering the combinatorial structure of (3) it was extremely helpful for us to have a graphical presentation as diagrams of chords and threads. To every term of the expansion (4) of an N-point function we associate a diagram as follows:

Definition B.1 (diagrammatic presentation). Draw N nodes on a circle, label them from b_0 to b_{N-1}. Draw a (grey solid) chord between b_r, b_s for every factor $G_{b_r b_s}$ in (4) and a (short-dashed for t, u even, long-dashed for t, u odd) thread between b_t, b_u for every factor $\frac{1}{E_{b_t}-E_{b_u}}$. The convention $t < u$ is chosen so that the diagrams come with a sign.

It was already known in [10] that the chords do not cross each other (using cyclic invariance (6)) and that the threads do not cross the chords (using (7)). But the combinatorial structure was not understood in [10] and no algorithm for a canonical set of chord diagrams could be given. The present paper repairs this omission.

The $N/2 = k+1$ chords in such a diagram divide the circle into $k+2$ pockets. The pocket which contain the arc segment between the designated nodes b_0 and b_{N-1} is by definition the root pocket P_0. Moving in the counter-clockwise direction, every time a new pocket is entered it is given the next number as index, as in Definition 5.1. The tree of these $k+2$ pockets, connecting vertices if the pockets border each other, is the pocket tree. A pocket is called even (resp. odd) if its index is even (resp. odd).

Inside every even pocket, the short-dashed threads (between even nodes) form the direct tree, the long-dashed threads (between odd nodes) form the opposite tree. Inside every odd pocket, the short-dashed threads (between even nodes) form the opposite tree, the long-dashed threads (between odd nodes) form the direct tree.

The sign τ of the diagram is given by

$$\tau(T) = (-1)^{\sum_{j=1}^{k+1} e_0^{(j)}}, \tag{30}$$

where $e_0^{(j)}$ is the first entry of the Catalan tuple corresponding to a pocket P_j. Indeed, for every pocket that is not a leaf or the root pocket, the chain of odd nodes starts with the highest index, which implies that every thread emanating from this node contributes a factor (-1) to the monomial (4) compared with the lexicographic order chosen there. In words: count for all pockets other than the root pocket the total number K of threads which go from the smallest node into the pocket. The sign is even (resp. odd) if K is even (resp. odd).

Figure 2 and 3 show nested Catalan tables and chord diagrams of the 4-point function and 6-point function, respectively. Figure 4 shows the chord diagram discussed in Example 5.4.

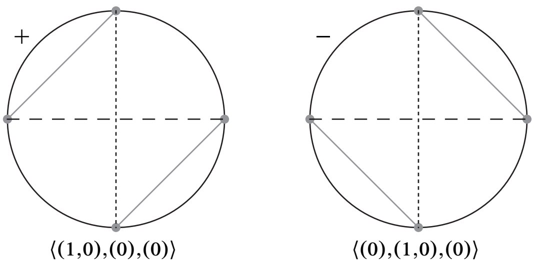

Figure 2. The two chord diagrams and nested Catalan tables of $G^{(0)}_{b_0b_1b_2b_3}$.

Now, that a visual way to study the recursion relation (3) has been introduced, it is much easier to demonstrate the concepts introduced in Sections 3 and 4.

Example B.2. The operation $\diamond$ is best demonstrated by an example:

$$\langle(1,0),(0),(0)\rangle\diamond\langle(0),(1,0),(0)\rangle = \langle(2,0,0),(0),(0),(1,0),(0)\rangle.$$

The corresponding chord diagrams are

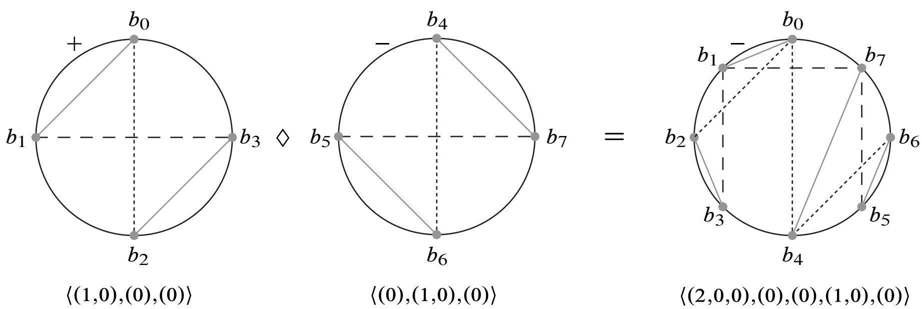

The diagrammatic recipe is to cut both diagrams on the right side of the designated node and paste the second into the first, where the counter-clockwise order of the nodes must be preserved. Then both designated nodes (here b_0, b_4) are connected by a short-dashed thread and nodes b_1 and $b_7 = b_{N-1}$ by a long-dashed thread.

To $\diamond$-decompose the nested Catalan table $\langle(2,0,0),(0),(0),(1,0),(0)\rangle$, we first $\circ$-factorise the zeroth pocket $(2,0,0)$ via (10). Here $\sigma_1\big((2,0,0)\big) = 1$ and, hence,

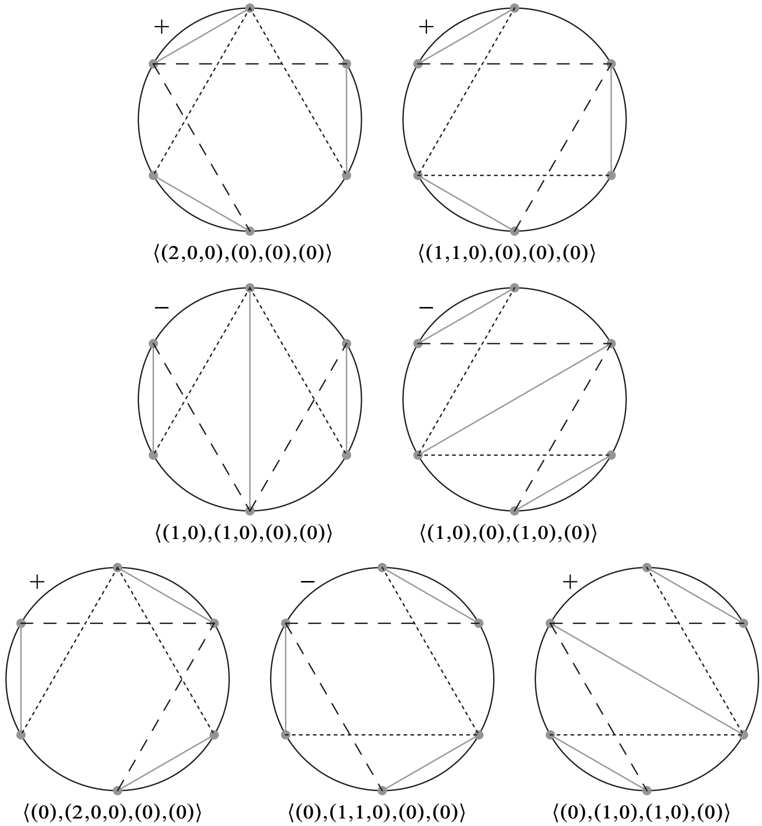

Figure 3. The seven chord diagrams and nested Catalan tables of $G^{(0)}_{b_0 b_1 b_2 b_3 b_4 b_5}$.

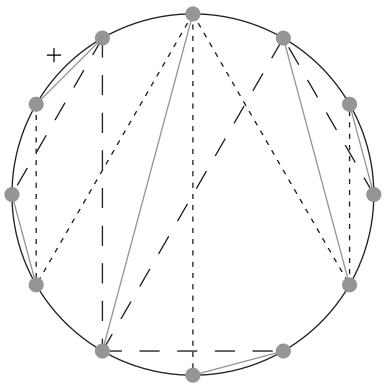

$\langle(2, 0, 0), (1, 1, 0), (0), (0), (0), (1, 0), (0)\rangle$

Figure 4. A chord diagram and nested Catalan table contributing to a planar 12-point function $G^{(0)}_{b_0 \ldots b_{11}}$. Pocket tree and all non-trivial direct and opposite trees have been given in Example 5.4.

$(2,0,0) = (1,0) \circ (0)$. Next, we evaluate the number $\hat{k}$ defined in (12). We have $1 + |\tilde{f}^{(0)}| = 1$ and $\sigma_1\big((3,0,0,1,0)\big) = 2$. Consequently, we get from Definition 4.2

$$\langle (2,0,0),(0),(0),(1,0),(0)\rangle = \langle (1,0),(0),(0)\rangle \diamond \langle (0),(1,0),(0)\rangle.$$

Example B.3. We employ the same example (with diagrams switched) to demonstrate the operation $\blacklozenge$. In terms of nested Catalan tables this becomes

$$\langle (0),(1,0),(0)\rangle \blacklozenge \langle (1,0),(0),(0)\rangle = \langle (0),(2,1,0,0),(0),(0),(0)\rangle,$$

for which the chord diagrams are

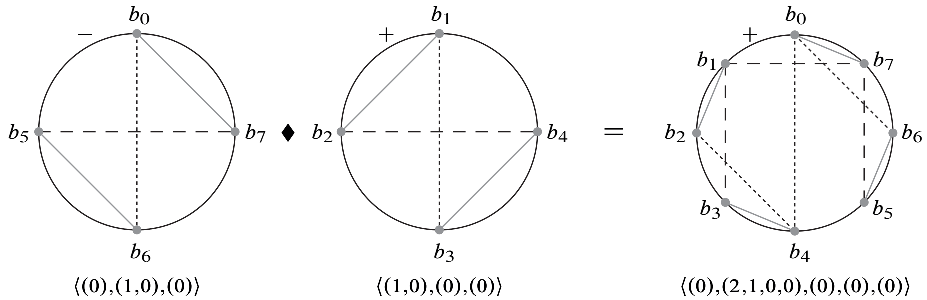

The diagrammatic recipe is to cut the first diagram on the left side of the designated node and the second diagram on the right side. Then paste the second into the first, where the counter-clockwise order of the nodes must be preserved. The threads in the second diagram switch long/short doing so. Then, the designated node of the first diagram is connected to the last node of the second by a short-dashed thread, the designated node of the second diagram is connected to the last node of the first diagram by a long-dashed thread.

Conversely, to $\blacklozenge$-decompose the nested Catalan table $\langle (0),(2,1,0,0),(0),(0),(0)\rangle$, we first $\bullet$-factorise the first pocket $e^{(1)} = (2,1,0,0)$ via (11). We have $e_0^{(1)} - 1 = 1$, hence consider $\sigma_1\big((2,1,0,0)\big) = 2$ and conclude $(2,1,0,0) = (1,0) \bullet (1,0)$. Next, we evaluate the number $\hat{l}$ in (13). With $|\tilde{e}^{(0)}| + |\tilde{e}^{(1)}| + 1 = 0 + 1 + 1 = 2$ the decomposition follows from $\sigma_2\big((1,3,0,0,0)\big) = 2$ and yields

$$\langle (0),(2,1,0,0),(0),(0),(0)\rangle = \langle (0),(1,0),(0)\rangle \blacklozenge \langle (1,0),(0),(0)\rangle.$$

Acknowledgements. We are grateful to an anonymous referee for an exceptionally comprehensive report which contained numerous suggestions that improved this paper.

Funding. This work was supported by the Deutsche Forschungsgemeinschaft via SFB 878 and the Cluster of Excellence "Mathematics Münster" ("Gefördert durch die Deutsche Forschungsgemeinschaft (DFG) im Rahmen der Exzellenzstrategie des Bundes und der Länder EXC 2044–390685587, Mathematik Münster: Dynamik–Geometrie–Struktur”).

References

[1] G. Borot and S. Shadrin, Blobbed topological recursion: properties and applications. *Math. Proc. Cambridge Philos. Soc.* **162** (2017), no. 1, 39–87 Zbl 1396.14031 MR 3581899

[2] J. Branahl, A. Hock, and R. Wulkenhaar, Blobbed topological recursion of the quartic Kontsevich model I: Loop equations and conjectures. 2020, arXiv:2008.12201

[3] J. Branahl, A. Hock, and R. Wulkenhaar, Perturbative and geometric analysis of the quartic Kontsevich model. *SIGMA Symmetry Integrability Geom. Methods Appl.* **17** (2021), paper no. 085 Zbl 07431224 MR 4312825

[4] E. Deutsch and M. Noy, Statistics on non-crossing trees. *Discrete Math.* **254** (2002), no. 1–3, 75–87 Zbl 0999.05018 MR 1909861

[5] B. Eynard, *Counting surfaces*. Prog. Math. Phys. 70, Birkhäuser, Basel, 2016 Zbl 1338.81005 MR 3468847

[6] B. Eynard and N. Orantin, Mixed correlation functions in the 2-matrix model, and the Bethe ansatz. *J. High Energy Phys.* (2005), no. 8, article no. 028 MR 2165818

[7] B. Eynard and N. Orantin, Invariants of algebraic curves and topological expansion. *Commun. Number Theory Phys.* **1** (2007), no. 2, 347–452 Zbl 1161.14026 MR 2346575

[8] H. Grosse, A. Hock, and R. Wulkenhaar, How Prof. Zeidler supported our research on exact solution of quantum field theory toy models. *Vietnam J. Math.* **47** (2019), no. 1, 93–112 Zbl 1414.81157 MR 3913852

[9] H. Grosse and R. Wulkenhaar, Progress in solving a noncommutative quantum field theory in four dimensions. 2009, arXiv:0909.1389

[10] H. Grosse and R. Wulkenhaar, Self-dual noncommutative ϕ^4-theory in four dimensions is a non-perturbatively solvable and non-trivial quantum field theory. *Comm. Math. Phys.* **329** (2014), no. 3, 1069–1130 Zbl 1305.81129 MR 3212880

[11] A. Hock and R. Wulkenhaar, Blobbed topological recursion of the quartic Kontsevich model II: Genus$=0$. 2021, arXiv:2103.13271

[12] M. Noy, Enumeration of noncrossing trees on a circle. In *Proceedings of the 7th Conference on Formal Power Series and Algebraic Combinatorics (Noisy-le-Grand, 1995)*, pp. 301–313, 180, 1998 Zbl 0895.05031 MR 1603749

[13] E. Panzer and R. Wulkenhaar, Lambert-W solves the noncommutative Φ^4-model. *Comm. Math. Phys.* **374** (2020), no. 3, 1935–1961 Zbl 1436.81091 MR 4076091

[14] R. P. Stanley, *Enumerative combinatorics.* Vol. 2, Cambridge Stud. Adv. Math. 62, Cambridge University Press, Cambridge, 1999 Zbl 0945.05006 MR 1676282

[15] The on-line encyclopedia of integer sequences, A001764. https://oeis.org/A001764

[16] The on-line encyclopedia of integer sequences, A006013. https://oeis.org/A006013

[17] W. T. Tutte, A census of planar maps. *Canadian J. Math.* **15** (1963), 249–271 Zbl 0115.17305 MR 146823

[18] R. Wulkenhaar, Quantum field theory on noncommutative spaces. In *Advances in noncommutative geometry*, pp. 607–690, Springer, Cham, 2019 Zbl 07217281 MR 4300561

Communicated by Abdelmalek Adbesselam

Received 26 April 2019.

Jins de Jong
TNO, Postbus 1416, 9701 BK Groningen, The Netherlands; jins.dejong@tno.nl

Alexander Hock
Mathematical Institute, University of Oxford, Andrew Wiles Building, Woodstock Road, Oxford OX2 6GG, United Kingdom; alexander.hock@maths.ox.ac.uk

Raimar Wulkenhaar
Mathematisches Institut, Westfälische Wilhelms-Universität, Einsteinstr. 62, 48149 Münster, Germany; raimar@math.uni-muenster.de